Cellular and Molecular Life Sciences

RESEARCH ARTICLE

Drosophila Nesprin-1 controls glutamate receptor density at neuromuscular junctions

Véronique Morel · Simon Lepicard · Alexandre N. Rey · Marie-Laure Parmentier · Laurent Schaeffer

Abstract   Nesprin-1 is a core component of a protein complex connecting nuclei to cytoskeleton termed LINC (linker of nucleoskeleton and cytoskeleton). Nesprin-1 is anchored to the nuclear envelope by its C-terminal KASH domain, the disruption of which has been associated with neuronal and neuromuscular pathologies, including autosomal recessive cerebellar ataxia and Emery–Dreifuss muscular dystrophy. Here, we describe a new and unexpected role of *Drosophila* Nesprin-1, Msp-300, in neuromuscular junction. We show that larvae carrying a deletion of Msp-300 KASH domain (*Msp-300$^{\Delta KASH}$*) present a locomotion defect suggestive of a myasthenia, and demonstrate the importance of muscle Msp-300 for this phenotype, using tissue-specific RNAi knock-down. We show that *Msp-300$^{\Delta KASH}$* mutants display abnormal neurotransmission at the larval neuromuscular junction, as well as an imbalance in postsynaptic glutamate receptor composition with a decreased percentage of GluRIIA-containing receptors. We could rescue *Msp-300$^{\Delta KASH}$* locomotion phenotypes by GluRIIA overexpression, suggesting that the locomotion impairment associated with the KASH domain deletion is due to a reduction in junctional GluRIIA. In summary, we found that Msp-300 controls GluRIIA density at the neuromuscular junction. Our results suggest that *Drosophila* is a valuable model for further deciphering how Nesprin-1 and LINC disruption may lead to neuronal and neuromuscular pathologies.

Keywords   *Drosophila* · GluRIIA · Msp-300 · Nesprin-1 · Neuromuscular junction

V. Morel (✉) · A. N. Rey · L. Schaeffer
Equipe Différenciation Neuromusculaire, CNRS, UMR5239, Ecole Normale Supérieure-Lyon, 46 allée d'Italie, 69364 Lyon Cedex 07, France
e-mail: veronique.morel@ens-lyon.fr

S. Lepicard · M.-L. Parmentier
Institut de Génomique Fonctionnelle, CNRS, UMR5203, 141 rue de la cardonille, 34094 Montpellier Cedex 05, France

S. Lepicard · M.-L. Parmentier
INSERM, U.661, Université Montpellier 1,2, Montpellier, France

L. Schaeffer
Université Lyon 1, Villeurbanne, France

L. Schaeffer
Centre de biotechnologies cellulaires, Hospices civils de Lyon, Lyon, France

Abbreviations

ANC-1	Nuclear anchorage protein-1
ARCA1	Autosomal recessive cerebellar ataxia
Dlg	Discs-large
EDMD	Emery–Dreifuss muscular dystrophy
ER	Endoplasmic reticulum
eEJC	Evoked excitatory junctional current
eEJP	Evoked excitatory junctional potential
GluRII	Glutamate receptor type II
IkB	Inhibitor of kappa B
KASH	Klarsicht/ANC-1/Syne homology
LINC	Linker of nucleoskeleton and cytoskeleton
MAGUK	Membrane-associated guanylate kinase
mEJC	Miniature excitatory junctional current
mEJP	Miniature excitatory junctional potential
MHC	Myosin heavy chain
Msp-300	Muscle-specific protein-300
NF-kB	Nuclear factor kappa-light-chain-enhancer of activated B cells

NMJ	Neuromuscular junction
RNAi	RNA interference
ROI	Region of interest
SR	Spectrin repeats
SSR	Subsynaptic reticulum
WT	Wild type

Introduction

Nesprins are conserved proteins characterized by a central rod of spectrin repeats (SR) and anchored to the outer nuclear membrane by a C-terminal KASH (Klarsicht/ANC-1/Syne homology) domain. Nesprins are core components of a protein complex termed LINC (for linker of nucleoskeleton and cytoskeleton, Fig. 1a), which is thought to provide a physical connection between the extracellular matrix, the cytoskeleton, and the nuclear content, and is now seen as a major player of nuclear function in cells [1–3].

Disruption of Nesprin-1, the largest of the four mammalian Nesprins, has been associated with impaired motor neuron innervation [4] and altered laminar structure formation in several brain regions, including the cerebellum [5]. The importance of Nesprin-1 in neurons was further illustrated by the identification of mutations resulting in deletion of Nesprin-1 KASH domain in patients suffering from autosomal recessive cerebellar ataxia ARCA1 [6]. Similar mutations leading to Nesprin-1 disconnection from the LINC complex were identified in patients with Emery–Dreifuss muscular dystrophy (EDMD) [7], an early onset muscular disease [8].

In mice, skeletal muscle fibers are large syncitia containing thousands of extrasynaptic nuclei evenly distributed along the fiber and 6–8 subsynaptic nuclei clustered below the neuromuscular junction [9]. Subsynaptic nuclei are dedicated to synaptic genes expression and their localization is essential for that function [9, 10]. Mice models showed that Nesprin-1 association with the nuclear envelope is required for myonuclei subcellular localization, in particular with respect to the neuromuscular junction, and for muscle function [4, 11–13]. These phenotypes echo observations made in EDMD patients. Yet the molecular mechanisms underlying Nesprin-1 function with respect to muscle physiology remain unknown. To tackle this question, we undertook to study the consequences of disconnecting Msp-300, the *Drosophila* Nesprin, from nuclei on muscle function.

Initially identified as a muscle-specific dystrophin-like protein [14], Msp-300 was shown, by bioinformatic analyses, to be the unique *Drosophila* ortholog of Nesprins, and then proposed, based on sequence comparisons, to be more closely related to Nesprin-1 [15]. We present here biological evidence that Msp-300 is a Nesprin-1. We show that Msp-300 localizes around nuclei in a KASH-dependent manner and is required for myonuclei anchoring. We then show that disconnecting Msp-300 from nuclei by deleting its KASH domain leads to a postsynaptic imbalance in glutamate receptor sub-units composition correlated with neuromuscular junction impairment and locomotion defects in larvae. We therefore propose that the study of Msp-300 function in muscle constitutes a valuable system to decipher the molecular mechanisms by which the LINC complex impacts on neuromuscular physiology.

Materials and methods

Genetics

Drosophila stocks were obtained or modified from stocks of the following sources: ; Msp-300$^{\Delta KASH}$/CyO,Dfd-YFP;;, w[1118];Df(2L)Exel6011/CyO;;, Elav-Gal4;UAS-Dicer2;,;;24B-Gal4;,;UAS-Dicer2;24B-Gal4;, from the Bloomington Stock Center, w1118, P{GD10317}v50192;;; (UAS-v50192 [16]) from the Vienna Drosophila RNAi Center.;MHC-GluRIIA::myc;; were gift from G. Davis (University of California),;GluRIIA[AD9]/CyO;; from A. DiAntonio (Washington University), ;;*ens^{swo}*, ap-DsRed/TTG; from M. Baylies (Sloan-Kettering Inst.). *Canton S* were used as WT control for locomotion and electrophysiology assays, *yw* for immunostainings. For RNAi experiments, females UAS-v50192 were crossed to males carrying the Gal4 construct or to CS males for controls. Flies were raised on standard cornmeal agar food and in natural day light cycle. For locomotion assays, cages were set up with agar plates with some active yeast paste. Flies laid eggs for 2 h and embryos were then aged at 25 °C before being processed.

Locomotion assays

For the global locomotion assay, 48 h after egg laying (AEL) old larvae were collected and washed in water. A single larva was placed at the center of an agar plate positioned above a 5 x 5 mm grid. Locomotion was manually tracked under the microscope (Discovery.V8, Zeiss) for 2 min and the number of squares crossed by the larva was scored. A picture of the larva was taken using a camera (AxioCam MRc5, Zeiss) coupled to the microscope and larval size was measured using Axiovision software. Global locomotion score was calculated as follows: Nb (squares) × 5,000/larval size (in μm). Global locomotion assays were performed at 22–23 °C.

For fine locomotion analysis, a 48 h AEL old larva was collected, washed, and placed on an agar plate. Time-lapse imaging (1 image/150 ms) of the locomotion of the larva was performed using a macroscope (Leica Z16 ApoA coupled
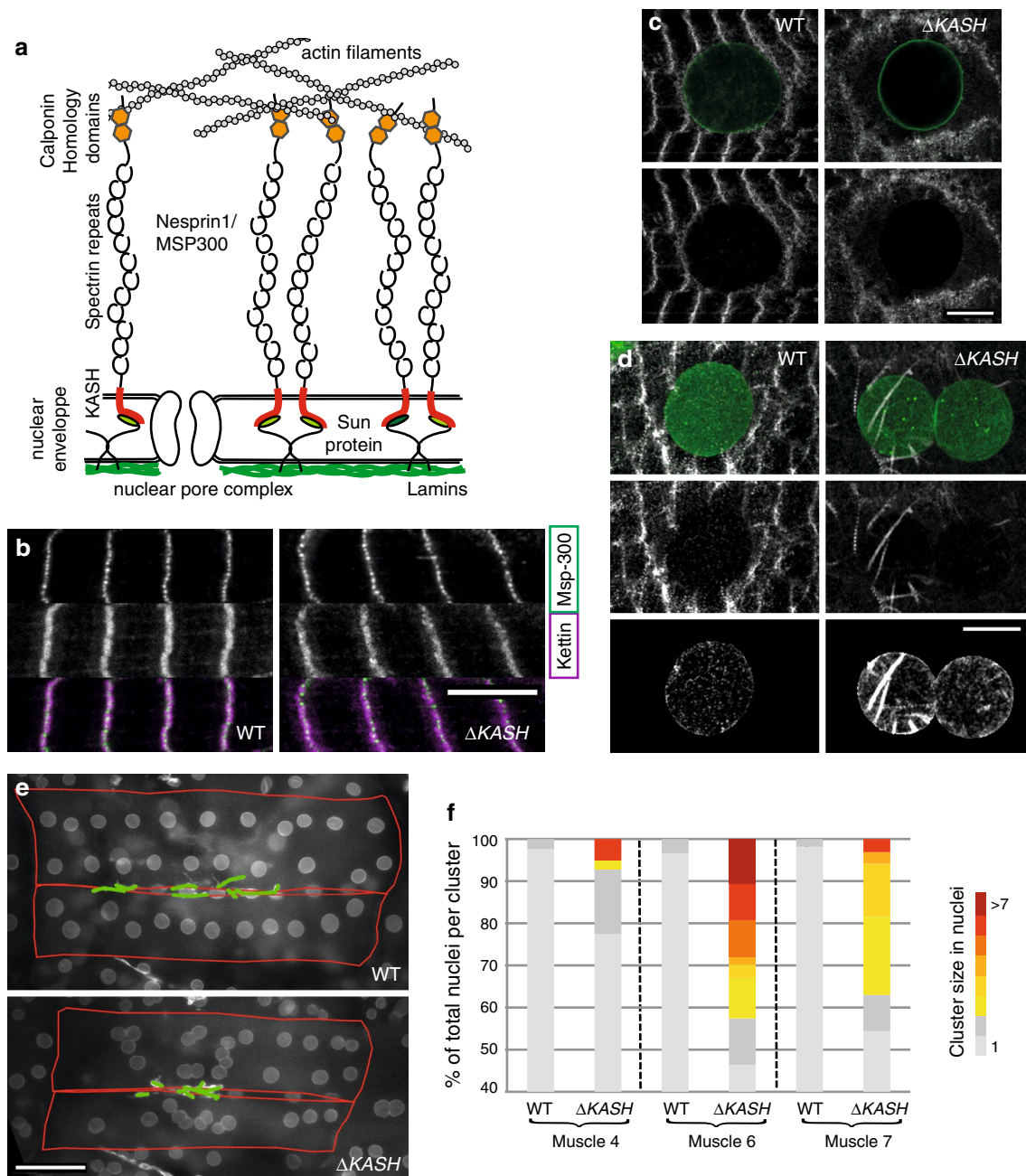
Fig. 1 Msp-300 subcellular localization and contribution to nuclei anchoring. **a** Schematic representation of the LINC complex. **b–d** Confocal images of WT and *Msp-300^{ΔKASH}* third-instar wandering larvae showing Msp-300 subcellular localization (in *grey*). **b** Msp-300 localizes at Z-bands (revealed by Kettin, D-Titin) in a punctate pattern in both WT (*left*) and *Msp-300^{ΔKASH}* (*right*) larvae. *Top panels* show Msp-300 staining, *middle panels* Kettin staining, and *lower panels* the overlay with Msp-300 in *green* and Kettin in *magenta*. **c, d** Perinuclear localization of Msp-300 in muscle 4. The nuclear envelope is labeled using an anti LaminA antibody (in *green*). The *lower panels* show Msp-300 staining alone. **c** Msp-300 is found apposed to the nuclear envelope. In *Msp-300^{ΔKASH,}* Msp-300 retracts from the nucleus, forming a ring disconnected from the nuclear envelope. **d** In WT larvae (*left panels*), Msp-300 localizes in puncta arranged in

strings and forming a light net at the surface of the fiber as shown on the *middle panel*. The *lower panel* is an enhanced image of the nucleus surface revealing the homogeneous web of Msp-300 staining. In *Msp-300^{ΔKASH}* (*right panels*), surface localization of Msp-300 is less regular and occasional spikes of Msp-300 can be observed (in 34 % of nuclei, $n = 47$). **e** Muscles 6 and 7 of WT and *Msp-300^{ΔKASH}* larvae showing muscle (in *red*) and NMJ (in *green*) outlines and nuclei (stained with anti LaminA, in *grey*). Nuclei are evenly spaced in WT larvae but clustered in *Msp-300^{ΔKASH}*. **f** Clustering quantification in fibers 4, 6, and 7, comparing WT and *Msp-300^{ΔKASH}* conditions and showing the percentage of total nuclei found isolated or in groups of two to more than seven nuclei. *Scale bars* in **b**, **c** and **d**: 10 μm, in **e**: 100 μm

to a Coolsnap ES2 camera and using a PlanApo 1× objective and Metamorph software). For each film, the number of frames spent in a given behavior was manually extracted. Sub-films were generated with the straight sequences. These were processed through ImageJ software: for each image, the outline of the larva was extracted, the position of its centroid and its Feret's diameter calculated. The data were then processed to obtain the instant speed and larval size (maximum value of Feret's diameter measured for that larva) and contraction amplitude (min Feret's diameter/max Feret's diameter). Acquisitions were performed at 22 °C.

In order to control for external stimuli, each assay included a group of control wild-type (WT) larvae that was used as a reference for the behavioral analysis.

Electrophysiology

Electrophysiology at the NMJ was done using two-electrode voltage-clamp (TEVC) methods as described previously [17]. Wandering third-instar larvae were dissected in cold hemolymph-like HL3.1 [18] saline solution without calcium [HL3 solution contained (in mM): 70 NaCl, 5 KCl, 4 $MgCl_2$ $6H_2O$, 10 $NaHCO_3$, 5 trehalose $2H_2O$, 115 sucrose, and 5 HEPES, pH 7.2]. After dissection, larvae were placed in an electrophysiological bath containing the HL3.1 solution with 0.45 mM $CaCl_2$. All recordings were made at a temperature between 16 and 18 °C from muscle 6 segment A3. Sharp borosilicate electrodes (made with Sutter instrument, model P-1000) with a resistance of 8–25 MΩ and filled with 3 M KCl were used for intracellular recordings. Evoked excitatory junctional currents (eEJCs) were stimulated with a glass suction electrode on the appropriate segmental nerve at a suprathreshold voltage level. All current recordings were done in voltage-clamped muscle (−60 mV) with Axoclamp 200B (molecular devices) and analyzed with Clampex and Clampfit 10.2 software.

Immunostainings

Wandering L3 larvae were dissected in HL3.1 Ca^{2+}-free medium and fixed 15 min in Bouin's fixative (for GluR stainings) or 20 min in 4 % paraformaldehyde. Larvae were extensively washed in PBS-0.1 % Triton X-100 (PBTx), blocked for 1 h in PBTx-0.1 % BSA, and incubated overnight at 4 °C with the primary antibodies. After several washes in PBTx-BSA, secondaries were added for 2 h at RT. The larvae were mounted in Vectashield (VectorLab). The following primary antibodies were generously provided by: anti-GluRIIC (rb, 1/5,000, [19]), anti-GluRIIB (rb, 1/2,500, [19]), anti-Dorsal (rb, 1/1,000; S. Wassermann), anti-Cactus (rb, 1/1,000; S. Wassermann), and anti-MSP300 (gp, 1/500, [14]). Anti Kettin (rat, MAC 155, 1/200) was obtained from Babraham Institute, anti-HRP-FITC (1/400)

from Jackson ImmunoResearch Europe, anti-myc (m, 9E10, 1/500) from Covance and Developmental Studies Hybridoma Bank provided for anti-GluRIIA (m, Corey Goodman, 1/50), anti-LaminA (m, P. Fischer, 1/200), anti-nc82 (m, E. Buchner 1/100), and anti-Dlg (m, C. Goodman, 1/200). Secondary antibodies were anti-gp-Alexa647 (1/1,000), anti-rabbit-Alexa647 (1/1,000), anti-rat-Alexa647 (1/500), phalloidin-Alexa555 (1/400) from Molecular Probes and anti mouse-Dylight488 (Jackson ImmunoResearch Europe, 1/2,000). In all the experiments involving comparisons of WT and $Msp-300^{\Delta KASH}$ backgrounds, larvae were processed identically and simultaneously.

Imaging

For nuclear clustering quantification, images of muscles 4, 6, and 7 of abdominal segments 3 and 4 were acquired using a Zeiss Plan neoFluar 20×/0.5 objective mounted on an AxioImager Z1 microscope (Zeiss) combined with a Coolsnap HQ camera (Photometric) and controlled by Metamorph software (Molecular Devices). For other immunofluorescent images, we used a Leica spectral confocal (DM 6000B microscope combined with a SP5 scanning device and a HCx PlanApo 60X/1.4 oil immersion objective from Leica) controlled by the Leica LAS-AF software. For NMJ analysis, Z sections were done every 0.2 μm through the entire junction of abdominal segments 3 and 4 muscle 4. WT and $Msp-300^{\Delta KASH}$ larvae of a given experiment were always processed with identical microscope and laser settings and during the same imaging session. We used an immersion oil-type LDF (index 1.515) and acquisitions were performed at 22 °C.

Image analysis

For nuclear clustering, nuclei with contacting nuclear envelope were scored as part of the same cluster. Percentage of clustering was measured as the number of nuclei in a given cluster's size to the total number of nuclei in that fiber.

Image analysis of NMJ was performed using ImageJ software. Synapse area was outlined either manually, based on GluRIIC staining, or with an automatic thresholding for HRP stainings. For fluorescence density measures, confocal sections restricted to the NMJ were projected using the sum projection from ImageJ, the total fluorescence within the synapse's ROI was measured and divided by synapse area. The percentage of GluRIIA-containing receptors was estimated by measuring the number of pixel costaining for GluRIIC and GluRIIA using Mander's colocalization coefficients [20] on a single confocal section. Measures of GluR densities and GluRIIA percentage were repeated, respectively, four and three independent times on 7–20 NMJs and gave comparable results.

RT-qPCR

Samples of 20–23 h AEL old staged embryos were collected, washed in water, and grinded in TRIzol (Invitrogen) for RNA extraction and purification. For each sample, 300 ng RNA, first treated by the TurboDNAse (Ambion), was reverse transcribed using random hexamers (Thermo-Scientific) and MMLV-H reverse transcriptase (Fermentas). Real-time PCR (Rotor Gene) was performed using primers specific for exon boundaries e31–e32 or *tbp-1* (as the reference gene) and SYBR green (QIAGEN) for amplicon detection and quantification. For comparison purposes, WT and UAS-v50192*/+;24B-Gal4/+* samples were always processed simultaneously. Relative mRNA levels were quantified as described in [21].

Statistics and graphical representations

Wilcoxon statistical test was performed with R. Box plot were done using 9th and 91st percentiles, histograms using average and SEM values.

Results

Msp-300 is the *Drosophila* homologue of Nesprin-1

Initially identified as a muscle-specific protein involved in *Drosophila* embryo muscle attachment, Msp-300 was proposed to be a dystrophin-like protein based on the presence of two CH domains together with spectrin repeats [14, 22]. Bioinformatic analyses then demonstrated the presence of additional 3prime exons, including one coding for a KASH domain, thereby identifying *Msp-300* as the unique *Drosophila* ortholog of Nesprins. Based on sequence comparisons, Msp-300 was proposed to be more closely related to Nesprin-1 [15]. In mice, Nesprin-1 is expressed in muscles, where it is anchored to the nuclear envelope of myonuclei [23–25]. Following KASH domain deletion, Nesprin-1 nuclear envelope localization is lost and muscle nuclei localization is altered with the exclusion of subsynaptic nuclei from the junctional area and extrasynaptic nuclei clustering [4, 12]. These features constitute the main hallmarks of Nesprin-1 and we investigated if Msp-300 shares with Nesprin-1 these functional properties in myofibers in which it is expressed.

We first documented Msp-300 subcellular localization in larval muscle, using an antibody targeting the central SRs rod of Msp-300 [14]. Msp-300 colocalizes with Kettin/D-Titin at Z-discs, where it displays a "beads on a string" pattern (Fig. 1b). Observation of Msp-300 localization in the depth of the muscle suggests that these strings actually form a sheet that penetrates within the sarcomeres at Z-discs.

When the perinuclear regions are observed, Msp-300 labeling indicates the presence of a dense web of filaments that surrounds muscle nuclei (Fig. 1d, see enhanced perinuclear staining on the bottom panel) and can be seen in close contact with the nuclear envelope in cross sections (Fig. 1c).

We then investigated Msp-300 subcellular localization in larvae homozygous for a genomic deletion removing *Msp-300* 3 last exons and therefore only expressing Msp-300 proteins lacking their KASH domain [26] (noted *Msp-300$^{\Delta KASH}$*). Msp-300 localization at Z-discs is not affected by Msp-300 KASH domain deletion (Fig. 1b). However, a strong disorganization of Msp-300 perinuclear distribution is observed, indicating a retraction of Msp-300 network from the nuclear envelope (Fig. 1c). Occasional spikes of Msp-300 over the nuclei are also seen in *Msp-300$^{\Delta KASH}$* larvae (Fig. 1d). These observations are in agreement with a role of the KASH domain in anchoring Msp-300 at the nuclear envelope.

Nesprin-1 [4, 12] and the *Caenorhabditis elegans* Nesprin-1 homolog ANC-1 [27] play a central role in nuclei localization in mammalian muscles and in *C. elegans* syncytial hypoderm, respectively. Since Msp-300 was predicted to be closely related to Nesprin-1, we investigated its contribution to myonuclei positioning. While nuclei are evenly spaced in wild-type muscles with <3 % of total nuclei found in clusters of two nuclei, *Msp-300$^{\Delta KASH}$* muscles are characterized by a strong nuclear clustering, with up to 54 % of nuclei found in clusters, some of which containing more than seven nuclei (Fig. 1e, f). Similar nuclear clustering is observed in larvae with muscle-specific expression of a Msp-300 RNAi or in larvae carrying a genomic deletion covering the 3prime half of the *Msp-300* locus together with the *Msp-300$^{\Delta KASH}$* allele (not shown). Thus, Msp-300 is required for myonuclei anchorage.

Altogether, these results constitute biological evidence that Msp-300 is the *Drosophila* homolog of Nesprin-1.

Deletion of Msp-300 KASH domain impairs larval locomotion

While investigating Msp-300 identity, we observed that *Msp-300$^{\Delta KASH}$* larvae were less mobile than WT larvae, suggesting a possible impairment of muscle function or stimulation. Larvae locomotion was therefore further investigated.

We first measured the total distance crawled by larvae in 2 min relative to their size (hereafter referred to as global locomotion) and observed a strong impairment of *Msp-300$^{\Delta KASH}$* locomotion capacities, with *Msp-300$^{\Delta KASH}$* global locomotion best score corresponding to 30 % of the score of WT larvae (Fig. 2a).

We then analyzed larvae movements using time-lapse imaging (Fig. 2d, e). Larvae display three types of movements: forward crawling (straight), turning, or stopping
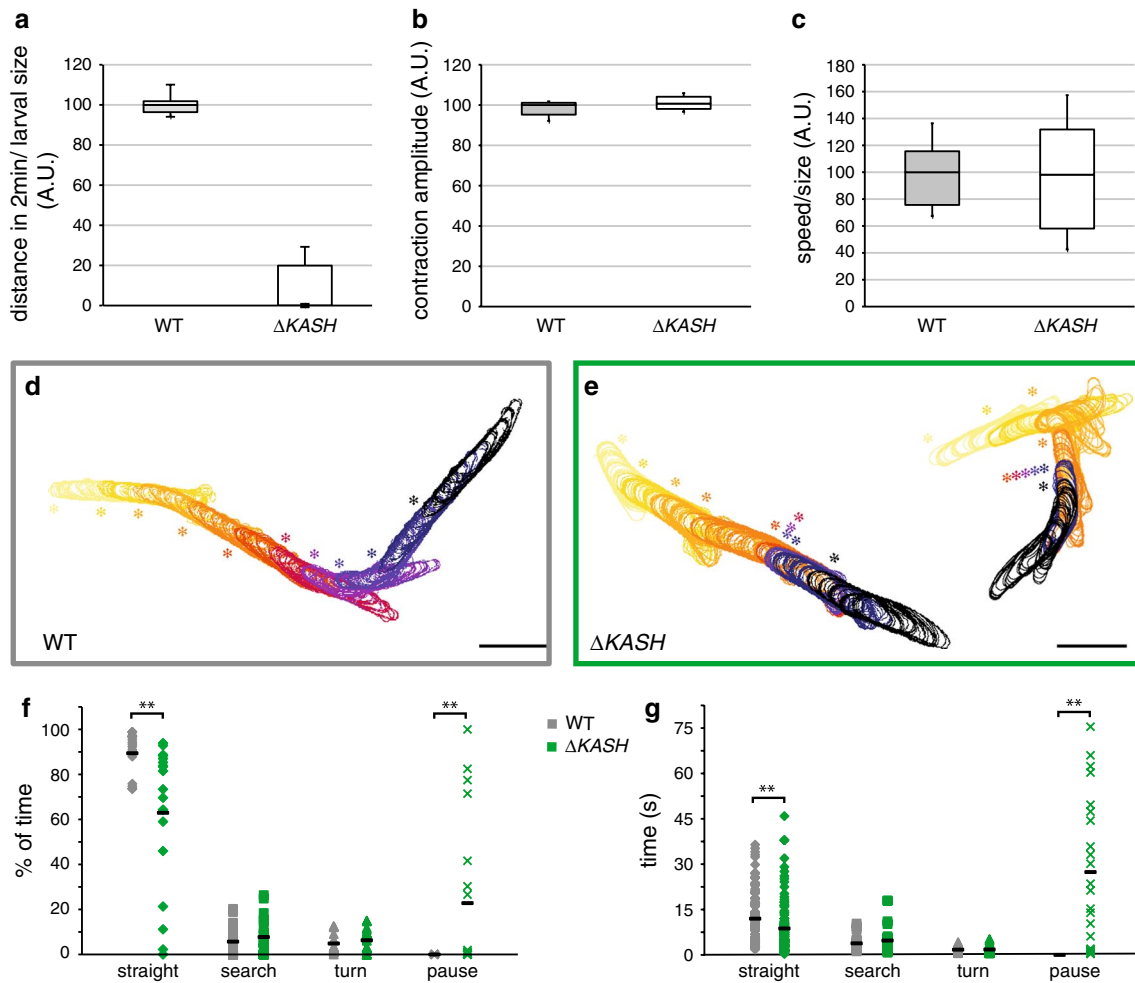
Fig. 2 *Msp-300$^{\Delta KASH}$* larvae show altered locomotion activity. **a** Box plot representation of the global displacement of 48 h AEL old larvae following 2 min of wandering relative to larval size (WT, $n = 13$, *Msp-300$^{\Delta KASH}$*, $n = 16$). **b–g** Fine locomotion analysis of WT and *Msp-300$^{\Delta KASH}$* larvae obtained by time-lapse imaging of 48 h AEL old larvae. **b** Contraction amplitude, i.e., ratio of the shortest to the longest size of the larva, directly reflecting longitudinal muscles contraction (WT, $n = 16$, *Msp-300$^{\Delta KASH}$*, $n = 16$). **c** Instant speed of the larva, extracted from pure forward movement sequences (*straight*) relative to larval size (WT, $n = 16$, *Msp-300$^{\Delta KASH}$*, $n = 19$). *Msp-300$^{\Delta KASH}$* values in **b** and **c** are not significantly different from WT (respectively, $p = 0.13$ and $p = 0.60$). (**a–c**) The values were normalized to the median value obtained with WT larvae. (**d–e**) Larval tracks extracted from 1 min long locomotion sequences representative of the WT and *Msp-300$^{\Delta KASH}$* behaviors. Locomotion was imaged by time-lapse imaging at a rate of 1 frame/150 ms. *Larvae outlines* are colored

by groups of 40 images (6 s) and superposed to show progression of the locomotion. A *star* marks the position of the first image of each group. Different behaviors can be observed on these tracks, including pauses shown by the superposition of stars (in **e**). *Scale bar* 1 mm. **f–g** Quantification of the different behaviors of WT (*grey*, $n = 16$) and *Msp-300$^{\Delta KASH}$* (*green*, $n = 19$) larvae, a *dark line* shows the median value for each category. **f** Total time spent adopting a given behavior represented as the percentage of the total locomotion sequence's length. A given larva will be represented by one point in each behavioral category. WT and *Msp-300$^{\Delta KASH}$* larvae significantly differ in the percentage of time spent in the straight and pause behaviors. **g** Duration of behavior sequences in seconds for each larva. Each larva will be represented by several points for each behavioral category. *Msp-300$^{\Delta KASH}$* larvae are characterized by significantly shorter straight and longer pause sequences than WT larvae. **p < 10^{-3}, Wilcoxon test

and exploring their environment by moving their head only (search). During straight sequences, the contraction amplitude, i.e., ratio of the shortest to the longest size of the larva, directly reflects the summed contraction of longitudinal muscles, while the instant speed is the combination of contraction amplitude and frequency. Impaired muscle contraction is thus expected to impair either parameter. WT and *Msp-300$^{\Delta KASH}$* larvae displayed similar contraction

amplitude (Fig. 2b) as well as identical instant speed relative to their size (Fig. 2c). Consistently, sarcomeric organization, as revealed by phalloidin staining (not shown) and Z-discs Msp-300 pattern (Fig. 1b), is normal in *Msp-300$^{\Delta KASH}$* larvae. Altogether, these results indicate that muscle organization and contractility is not affected by *Msp-300$^{\Delta KASH}$* mutation and that the overall locomotion defects we observed is not due to intrinsic muscle contractility defects.

WT larvae spend 89 % of their time going straight and occasionally turn (5 %) or search (6 %) (Fig. 2d, f). *Msp-300$^{\Delta KASH}$* larvae spend the same time either turning or searching (6 and 8 % of total time, respectively, Fig. 2f), but in contrast to the constant activity of WT larvae, *Msp-300$^{\Delta KASH}$* larvae regularly stay completely immobile (pause behavior, 23 % of total time; see also the superposition of frames in the locomotion tracks of *Msp-300$^{\Delta KASH}$* larvae, Fig. 2e). Accordingly, *Msp-300$^{\Delta KASH}$* larvae spend significantly less time moving forward (63 % of total time, $p = 2.10^{-4}$, Wilcoxon test). The duration of individual straight sequences in *Msp-300$^{\Delta KASH}$* larvae is also significantly shorter when compared to WT (an average of 8.7 s compared to 12 s, $p = 8.10^{-4}$, Wilcoxon test, Fig. 2g). These shorter forward sequences coupled to pauses explain the global locomotion defect described above. Importantly, the frequent pauses was suggestive of muscle fatigability.

Msp-300 impairment in muscle affects synapse function

In mammals, pathologic muscle fatigability is referred to as myasthenia. Myasthenic syndromes are typically associated with neurotransmission defects due to alterations of the neuromuscular synapse.

To test the contribution of Msp-300 to synapse function, we first investigated if the locomotion defects could be attributed to pre- or postsynaptic defects and subjected larvae with neuron or muscle-specific Msp-300 RNAi knock-down to global locomotion tests. RNA-seq analysis of *Msp-300* locus led to prediction of 11 isoforms for *Msp-300*, some containing the KASH domain while others did not, all KASH domain-containing isoforms sharing the ten last exons (# 32 to 41, http://flybase.org/reports/FBgn0261836.html). To mimic the genomic KASH domain deletion, we specifically targeted the KASH domain-containing isoforms using an RNAi directed against the exon 32. This RNAi was expressed either in neurons or in muscles using the Gal4/UAS system [28] (with the Elav-Gal4 and the 24B-Gal4 drivers, respectively). Efficiency of the RNAi was first confirmed by RT-qPCR (exon32 containing RNAs are at least three times less abundant following muscle-specific RNAi compared to control) and by Msp-300 immunostaining (Suppl Fig.). We then compared the performances of the different genotypes in the global locomotion assay (Fig. 3a). Larvae expressing the RNAi in neurons do not markedly differ from the controls (distance$^{Elav-Gal4}$ = 107 % distance^{control}). Conversely, a strong effect of the muscle-specific RNAi can be observed on larval locomotion abilities (distance$^{24B-Gal4}$ = 78 % distance^{control}, $p = 10^{-3}$, Wilcoxon test). This effect is specific of the RNAi since RNAi enhancement by over-expression of Dicer2 [29] further decreases the distance covered by larvae (distance$^{UAS-Dicer2;24B-Gal4}$ = 22 % distance^{control},

$p = 2.10^{-4}$, Wilcoxon test). In agreement with the muscle-specific expression of Msp-300 [14] (Fig. 1), these results all together suggest that Msp-300 is required for locomotion in the postsynaptic element.

We then directly tested whether Msp-300 is required for normal synaptic function by subjecting WT and *Msp-300$^{\Delta KASH}$* wandering third-instar larvae to electrophysiological analysis. Intracellular two electrodes voltage clamp recordings at the larval NMJs were performed on muscle 6 of segments A3. The amplitude of miniature excitatory junctional currents (mEJCs) was similar in *Msp-300$^{\Delta KASH}$* and WT larvae (mEJC: WT: 0.80 ± 0.05 nA; *Msp-300$^{\Delta KASH}$*: 0.80 ± 0.04 nA, mean ± SEM; $n = 10$) (Fig. 3b, d). However, when we analyzed evoked excitatory junctional currents (eEJCs), we observed a clear decrease in the *Msp-300$^{\Delta KASH}$* mutants compared to control larvae (WT: 56.7 ± 2.6 nA; *Msp-300$^{\Delta KASH}$*: 40.9 ± 3.4 nA, mean ± SEM; $n = 10$; Wilcoxon test, $p = 0.0029$) (Fig. 3c, e). Similarly, quantal content (eEJC/mEJC), often considered as the number of released vesicles upon stimulation, showed an approximate 29 % reduction in *Msp-300$^{\Delta KASH}$* compared to WT (WT: 72.9 ± 4.6; *Msp-300$^{\Delta KASH}$*: 52.4 ± 5.2 mV, mean ± SEM; $n = 10$; Wilcoxon test, $p = 0.0115$, Fig. 3f). Thus, synaptic function is impaired upon Msp-300 KASH domain deletion.

Msp-300 controls GluRIIA abundance at the synapse

Since Msp-300 is required in the postsynaptic compartment, we further investigated the subcellular correlates of altered neurotransmission by looking at postsynaptic receptors. Indeed, modification of postsynaptic receptor subunit composition can modify synapse physiology [30, 31].

Five glutamate receptor subunits are present at the *Drosophila* NMJ. They associate to form two types of heterotetrameric receptors [32]. The A and B types of glutamate receptors share the GluRIIC, GluRIID, and GluRIIE subunits and contain respectively either GluRIIA or GluRIIB subunit [19, 30–34]. Deletion of both *gluRIIA* and *gluRIIB* genes leads to embryonic lethality. This lethality can be rescued by expression of either *gluRIIA* or *gluRIIB*, showing that either gene is sufficient for viability [31]. DiAntonio et al. [31] showed that A- and B-type receptors generate identical channel current amplitude but trigger different time constant of desensitization and proposed a model in which A- and B-type receptor density is a determinant of the postsynaptic response.

We therefore evaluated the amount of the different types of glutamate receptors in *Msp-300$^{\Delta KASH}$* and WT larvae by immunostaining. GluRIIA labeling reveals a punctuate distribution of GluRIIA within the NMJ in WT larvae, as previously described [30, 32], as well as in *Msp-300$^{\Delta KASH}$* larvae (Fig. 4a). Interestingly, we observe a significant
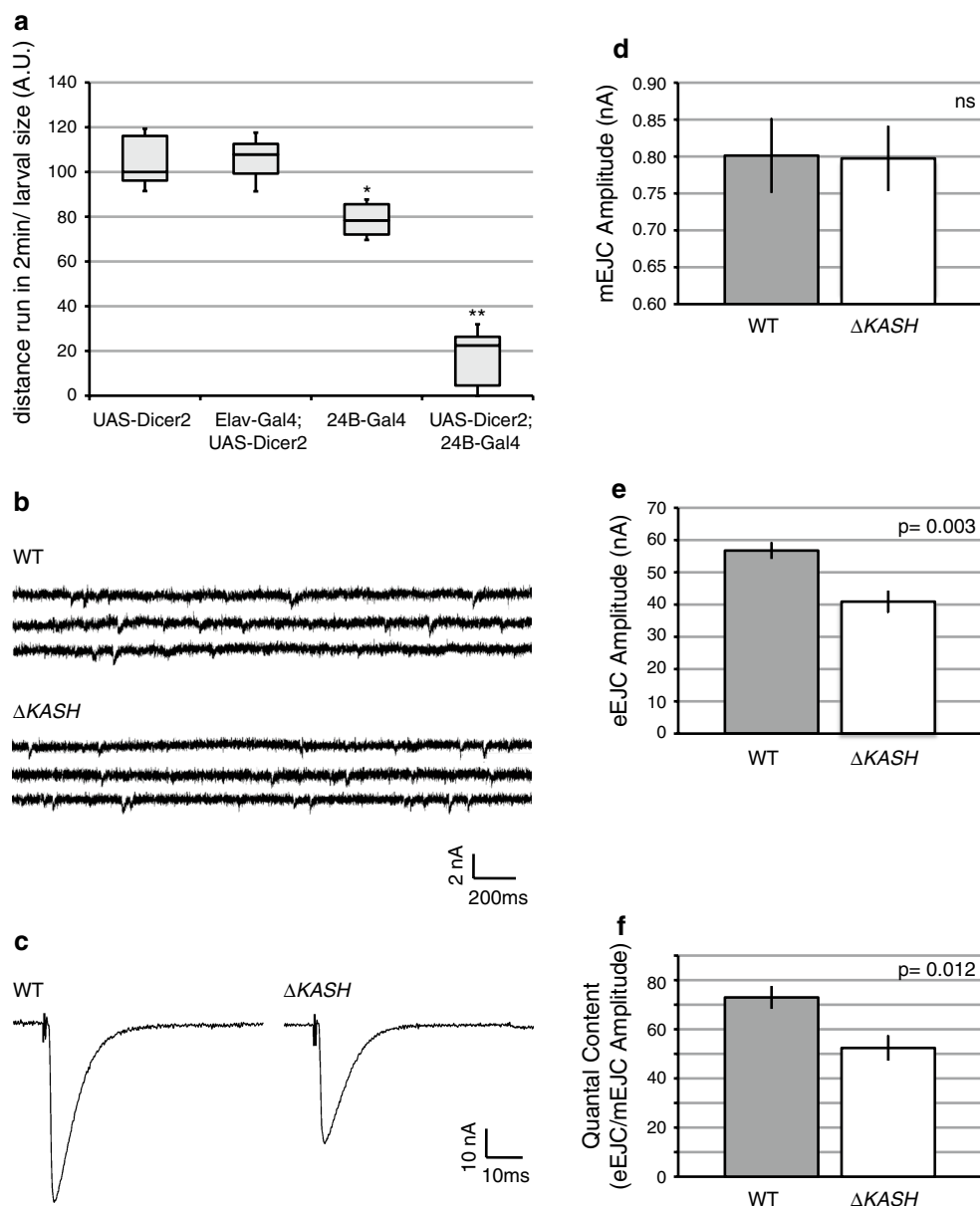
Fig. 3 Msp-300 KASH domain deletion results in postsynaptic alteration of NMJ function. **a** Comparison of the global displacement relative to larval size following 2 min of wandering of 48 h AEL old control larvae (;UAS-Dicer2;, $n = 7$) and 48 h AEL old larvae with either neuron (Elav-Gal4; UAS-Dicer2;, $n = 14$) or muscle (24B-Gal4, $n = 16$ and UAS-Dicer2; 24B-Gal4, $n = 14$)-specific RNAi knock-down of *Msp-300*. For the ease of comparison, the median value obtained for control larvae was adjusted to 100. While neuron-specific knock-down of *Msp-300* does not alter larval crawling capacities, we observe a marked decrease in the distance/larval size for the 24B-Gal4 progeny. This decrease is enhanced by the potentiation of RNAi upon

Dicer2 expression (UAS-Dicer2; 24B-Gal4 progeny), hence showing the specificity of the RNAi knock-down (78 and 22 % of control distance/size, respectively, Wilcoxon test, *$p = 0.0012$, **$p = 0.0003$). **b–f** Voltage clamp recordings from muscle 6 of abdominal segment 3 of WT and *Msp-300$^{\Delta KASH}$*. Representative traces of spontaneous neurotransmitter release (**b**) and evoked synaptic transmission (**c**) recorded from WT and *Msp-300$^{\Delta KASH}$* larvae. **d** The amplitude of mEJCs is not different in *Msp-300$^{\Delta KASH}$* and WT (Wilcoxon test, $p = 0.79$) while eEJCs amplitude (**e**) and quantal content (**f**, eEJC/mEJC) are significantly reduced in *Msp-300$^{\Delta KASH}$* when compared to WT (Wilcoxon test, $p = 0.0028$ and $p = 0.0115$, respectively)

decrease in GluRIIA fluorescence density in *Msp-300$^{\Delta KASH}$* compared to WT larvae (Fig. 4b).

To test if the total amount of postsynaptic receptors was modified, the fluorescence density measurements were repeated using an antibody directed against

one of the shared subunit, here GluRIIC. No difference in GluRIIC fluorescence density could be observed between *Msp-300$^{\Delta KASH}$* and WT larvae (Fig. 4c), therefore indicating that the total number of receptors is not affected by KASH domain deletion. The relative decrease in A-type
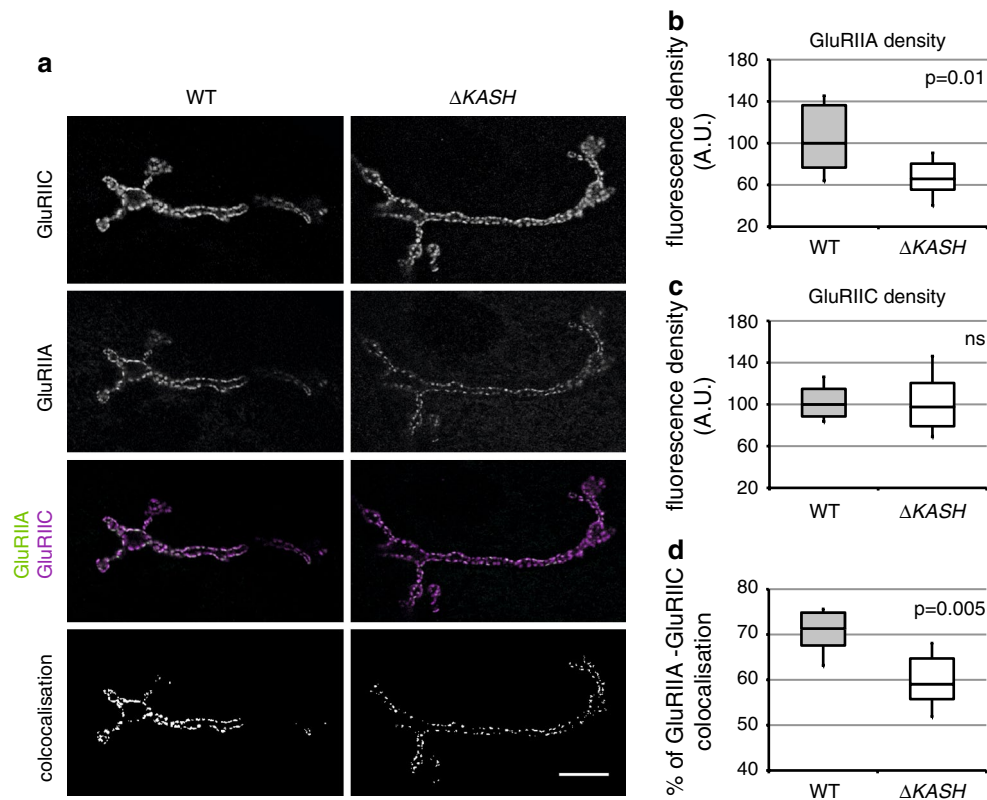
Fig. 4 Composition in glutamate receptors is altered in *Msp-300^(ΔKASH)* larvae. **a** Fiber 4 of WT and *Msp-300^(ΔKASH)* wandering third instar were labeled with GluRIIC (*top panels* and in *magenta* in the third) and GluRIIA (*second panels*, *green* in the third) to quantify the proportion of GluRIIA-containing receptors at the NMJ. *Bottom panels* show IIC dots colocalizing with IIA. **b** Representative measures of GluRIIA density in WT and *Msp-300^(ΔKASH)* showing fluorescence density of GluRIIA staining relative to WT median value. We observe a significant decrease in GluRIIA density in *Msp-300^(ΔKASH)* (med = 65.8 % of control, $n = 14$) compared to WT ($n = 10$; Wil-coxon test, $p = 0.01$) (experiment repeated four times). **c** Measure of GluRIIC density in WT and *Msp-300^(ΔKASH)* showing GluRIIC fluorescence density relative to WT median value. We did not observe any significant difference between WT ($n = 32$) and *Msp-300^(ΔKASH)* ($n = 34$). **d** Representative quantification of GluRIIA-containing receptors given by Mander's colocalization coefficient of GluRIIC and GluRIIA and showing a significant decrease in the proportion of A-type GluR at *Msp-300^(ΔKASH)* NMJ (59 %, $n = 8$ vs. 71 % in WT, $n = 12$; Wilcoxon test, $p = 0.005$). *Scale bar* 10 μm

receptors was further confirmed by direct evaluation of the GluRIIA/GluRIIC ratio after double staining. The percentage of GluRIIA-containing receptors was evaluated by measuring the proportion of GluRIIC-positive puncta that were also labeled with GluRIIA (Fig. 4a, see the *bottom panels* for colocalizations). KASH domain deletion results in a significant decrease in the percentage of GluRIIA-containing receptors at the NMJ (Fig. 4d).

In conclusion, the overall density of glutamate receptors at the NMJ is conserved in *Msp-300^(ΔKASH)* larvae, but the percentage of A-type receptors is decreased in *Msp-300^(ΔKASH)* larvae when compared to WT larvae.

GluRIIA rescue restore normal locomotion in Msp-300^(ΔKASH) larvae

gluRIIA inactivation in larvae causes impaired neuromuscular transmission with decreased miniature and evoked excitatory junctional potentials (mEJP and eEJP) [31]. These larvae also present an altered locomotion activity with short phases of straight movement and frequent pauses [35]. Both phenotypes are very similar to the ones we describe here for *Msp-300^(ΔKASH)* larvae. We thus investigated the possibility that *Msp-300^(ΔKASH)* larvae locomotion defects could be caused by reduced GluRIIA abundance.

We first compared the locomotion activity of *Msp-300^(ΔKASH)* larvae to that of larvae with reduced expression of *gluRIIA* (heterozygous for a deletion of the *gluRIIA* locus, *gluRIIA^(AD9)*/+). As shown in Fig. 5a, *Msp-300^(ΔKASH)* and *gluRIIA^(AD9)*/+ behave identically, presenting the same decrease in global locomotion.

We next evaluated if the *Msp-300^(ΔKASH)* locomotion defects could be rescued by muscle-specific over-expression of *gluRIIA* (using a MHC-GluRIIA::myc transgene). We first controlled the efficiency of the MHC-GluRIIA::myc transgene to drive GluRIIA expression
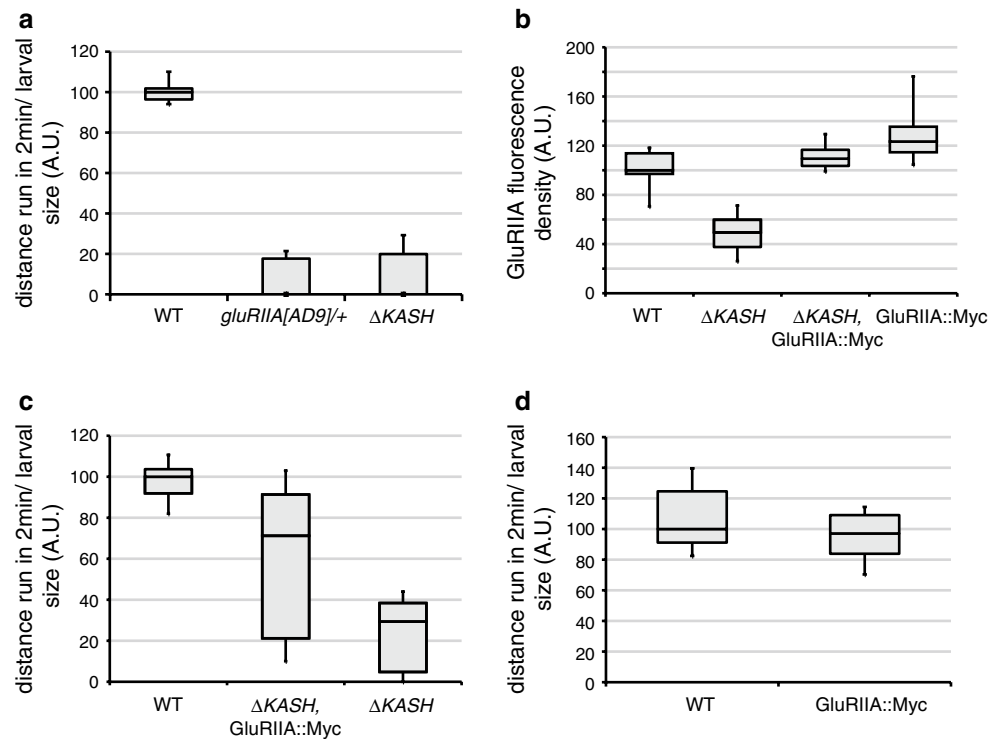
Fig. 5 GluRIIA junctional decrease in *Msp-300^ΔKASH* larvae results in locomotion impairment. **a**, **c**, **d** Distance run in 2 min by 48 h AEL old larvae relative to larval size. **a** Comparison of global locomotion of WT (*n* = 13), *Msp-300^ΔKASH* (*n* = 15), and *gluRIIA[AD9]/+* (*n* = 16) larvae. Larvae carrying a single copy of *gluRIIA* gene behave as *Msp-300^ΔKASH* larvae. **b** Comparison of fluorescence density of GluRIIA staining in WT, *Msp-300^ΔKASH*, *Msp-300^ΔKASH*, MHC-GluRIIA::myc and MHC-GluRIIA::myc. Muscle overexpression of GluRIIA rescues GluRIIA fluorescence density of *Msp-300^ΔKASH* larvae to WT levels. GluRIIA fluorescence density of MHC-GluRIIA::myc do not differ from WT levels, suggesting that GluRIIA is not limiting in WT conditions. **c** Global locomotion of *Msp-300^ΔKASH* larvae over-expressing *gluRIIA* specifically in muscles (*Msp-300^ΔKASH*, MHC-GluRIIA::myc, *n* = 22) compared with distance traveled by WT (*n* = 22) and *Msp-300^ΔKASH* (*n* = 22) larvae. Distance values of *Msp-300^ΔKASH*, MHC-GluRIIA::myc larvae significantly differ from values of WT (Wilcoxon test, *p* = 0.005) or *Msp-300^ΔKASH* larvae (*p* = 0.02). Sixty percent of the over-expressing larvae perform better than *Msp-300^ΔKASH* larvae, therefore showing a significant rescue of their locomotion abilities. **d** WT (*n* = 24) and GluRIIA overexpressing larvae (MHC-GluRIIA::myc, *n* = 26) perform identically in global locomotion tests, showing that GluRIIA is not limiting in WT conditions (Wilcoxon test, *p* = 0.1932)

in WT and *Msp-300^ΔKASH* larvae by measuring synaptic GluRIIA density. Junctional GluRIIA density is restored to WT levels in *Msp-300^ΔKASH* larvae carrying the MHC-GluRIIA::myc transgene (Fig. 5b). In addition, we observe a significant rescue of the locomotion activity of *Msp-300^ΔKASH* larvae over-expressing GluRIIA::myc (Fig. 5c) when compared to *Msp-300^ΔKASH* larvae. These results show that GluRIIA is limiting in *Msp-300^ΔKASH* larvae. Remarkably, the rescue of *Msp-300^ΔKASH*larvae by MHC-GluRIIA::myc was not complete and while 60 % of the *Msp-300^ΔKASH*, MHC-GluRIIA::myc larvae presented a significant rescue of their locomotion activity when compared to *Msp-300^ΔKASH* larvae (Wilcoxon test, *p* = 0.01), 40 % of the *Msp-300^ΔKASH*, MHC-GluRIIA::myc larvae still behaved like the *Msp-300^ΔKASH* mutants (Fig. 5c).

Two hypotheses can be proposed to explain the failure of GluRIIA::myc overexpression to rescue the locomotion activity in some of the *Msp-300^ΔKASH* larvae: either the timing of GluRIIA::myc overexpression does not match with endogenous GluRIIA expression, or GluRIIA::myc present an altered activity when compared to the endogenous GluRIIA and thus only partially rescue GluRIIA activity deficit in *Msp-300^ΔKASH* larvae. Our control experiment in Fig. 5d suggests that GluRIIA::myc activity does not differ from endogenous GluRIIA activity. Indeed, if this were the case, WT larvae carrying the MHC-GluRIIA::myc transgene should present a locomotion phenotype, which is not the case, WT and MHC-GluRIIA::myc larvae behaving identically in the global locomotion test. Hence, the partial penetrance of the locomotion rescue in *Msp-300^ΔKASH*, MHC-GluRIIA::myc larvae could be explained by differences in time or level of expression between endogenous and over-expressed GluRIIA.

We further analyzed what was the level of expression of GluRIIAmyc in control and *Msp-300^ΔKASH* mutants. We had performed GluRIIA stainings and shown that
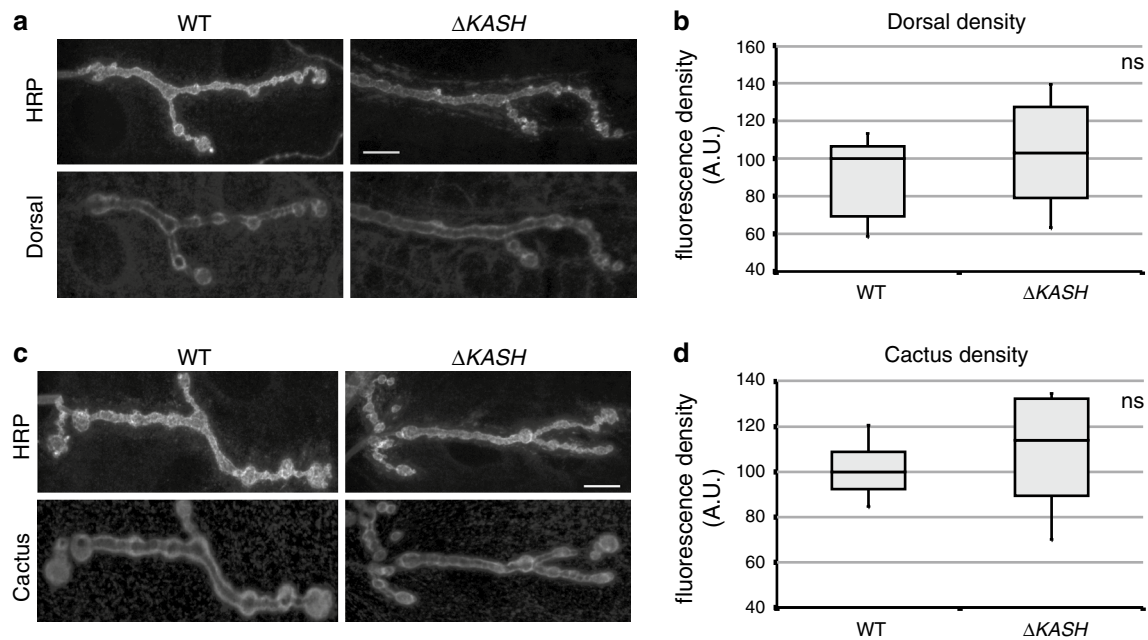
Fig. 6 Dorsal and Cactus sub-synaptic localizations are not affected by Msp-300 KASH domain deletion. Fiber 4 of WT (*left panels*) and *Msp-300$^{\Delta KASH}$* (*right panels*) wandering third-instar larvae labeled with Dorsal (**a**) and Cactus (**c**) together with HRP to show neuromuscular junction extent. Representative measures of Dorsal (**b**) and Cactus (**d**) fluorescence densities in WT and *Msp-300$^{\Delta KASH}$* relative to WT median value. We did not observe any significant difference between WT and *Msp-300$^{\Delta KASH}$* larvae neither in Dorsal (WT, $n = 8$, *Msp-300$^{\Delta KASH}$*, $n = 9$, Wilcoxon test, $p = 0.32$), or in Cactus fluorescence densities (WT, $n = 8$, *Msp-300$^{\Delta KASH}$*, $n = 9$, Wilcoxon test, $p = 0.96$). *Scale bar* 10 μm. The experiment was repeated three times for each staining

GluRIIA density was restored to normal in *Msp-300$^{\Delta KASH}$*, MHC-GluRIIA::myc larvae (Fig. 5b). We further evaluated the synaptic density of the over-expressed GluRIIA by measuring junctional myc density. myc density did not significantly differ between MHC-GluRIIA::myc and *Msp-300$^{\Delta KASH}$*, MHC-GluRIIA::myc larvae (data not shown). Hence, there is no difference in the expression levels of GluRIIA and GluRIIA::myc that could explain why the rescue by GluRIIA::myc is partial.

In conclusion, we show that, GluRIIA amount is limiting in *Msp-300$^{\Delta KASH}$* larvae but not in WT ones and the locomotion phenotype of *Msp-300$^{\Delta KASH}$* larvae is, at least partly, due to decreased GluRIIA abundance at the NMJ.

Msp-300 controls GluRIIA density independently of Dorsal or Cactus

Several proteins have been involved in glutamate receptors localization at the neuromuscular junction. Some, like the MAGUK protein Discs-large (Dlg), have been shown to specifically control type-B, but not type-A, synaptic glutamate receptor density [36]. Others, like *Drosophila* NF-κB and IκB, Dorsal and Cactus, contribute to GluRIIA synaptic density without affecting GluRIIB [37, 38]. We thus investigated if Msp-300 could act through one of these proteins to control GluRIIA synaptic localization.

Mutations in *dorsal* or *cactus* result in decreased GluRIIA density at the NMJ [38]. Since Dorsal and Cactus localize at the subsynaptic reticulum (SSR) of muscle fibers and *dorsal* or *cactus* mutations leading to decreased GluRIIA density are also associated with decreased SSR localization of Cactus [37], we wondered if Msp-300 could indirectly control GluRIIA density by modulating Dorsal or Cactus postsynaptic localization. However, no difference of Dorsal or Cactus NMJ fluorescence densities could be detected between *Msp-300$^{\Delta KASH}$* and WT larvae (Fig. 6), therefore excluding an indirect effect of Msp-300 on GluRIIA density via Dorsal or Cactus.

Locomotion impairment and nuclei clustering are disconnected phenotypes

Several studies reported a correlation between muscular impairment and myonuclei clustering. In agreement with the phenotypes we describe here for *Msp-300$^{\Delta KASH}$*, mice carrying a deletion of Syne1 KASH domain, used as a model for EDMD, present an important clustering of extrasynaptic nuclei [4, 12] together with decreased performances in treadmill running assays [13]. Similarly, mutations of the KASH-containing protein Klarsicht result in nuclei clustering in *Drosophila* larval fibers and impaired locomotion performances [39]. Our results, together with
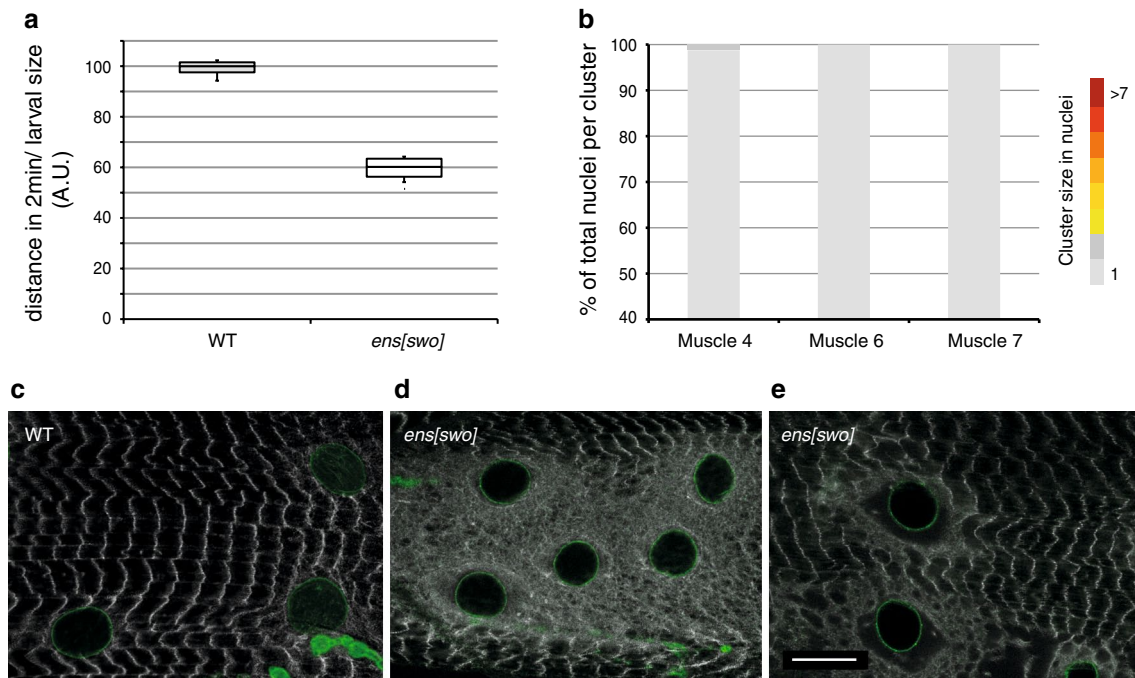
Fig. 7 ens^{swo} mutants present locomotion defects together with altered Msp-300 localization but no nuclei clustering. **a** Box plot representation of the global displacement of 48 h AEL old WT and ens^{swo} larvae following 2 min of wandering relative to larval size. Two independent tests including eight larvae per genotype were performed. In both tests, ens^{swo} larvae covered a distance corresponding to <60 % of the distance covered by WT larvae ($p < 10^{-3}$, Wilcoxon test). **b** Clustering quantification in muscles 4, 6, and 7 of ens^{swo} third-instar larvae and showing the percentage of total nuclei found isolated or in groups of two to more than seven nuclei. We analyzed 83 fibers from 11 larvae and only found four of the 1,150 nuclei counted in clusters of two (<2 % of the muscle four nuclei counted). Thus, there is no nuclei clustering in ens^{swo} third-instar larvae. **c–e** Subcellular localization of Msp-300 (*grey*) in WT (**c**) and ens^{swo} (**d**, **e**) muscle 4 of third instar larvae. While Z-band localization of Msp-300 appears normal in ens^{swo} mutants, Msp-300 perinuclear organization is altered. In all fibers, we observe a disorganized Msp-300 staining above the sarcomeres in the region surrounding the nuclei (labeled by LaminA in *green*, compare **c** and **e**). In addition, we observed in some fibers a gap in Msp-300 staining around the nuclei, which is very similar to Msp-300 organization observed in Msp-$300^{\Delta KASH}$ mutants (compare **c** and **d**, see Fig. 1c). *Scale bar* 20 μm

these observations, raise the question of the relative contribution of nuclei clustering vs. Msp-300 localization in the observed junctional/locomotion phenotype of Msp-$300^{\Delta KASH}$ larvae.

In an attempt to independently investigate the contributions of nuclei clustering and Msp-300 mislocalization to the locomotion impairment, we first turned to *klarsicht* mutants. Elhanany-Tamir et al. [39] described an alteration of Msp-300 subcellular localization in *klarsicht* mutants. However, the occurrence of both nuclei clustering and alteration of Msp-300 subcellular localization in these mutants does not allow us to discriminate between their relative contribution to the locomotion phenotype.

We then investigated the relative contributions of nuclei clustering and Msp-300 mislocalization in ens^{swo} mutants. ens^{swo} was identified by Metzger et al. [40] as a major factor of myonuclear positioning during muscle development. Metzger et al. described an alteration of the locomotion of third-instar ens^{swo} larvae together with an irregular spacing of the myonuclei. In order to compare ens^{swo} and Msp-$300^{\Delta KASH}$ mutants, we first subjected ens^{swo} larvae to our global locomotion test. As shown in Fig. 7a, 48 h AEL old ens^{swo} larvae cover in 2 min only 60 % of the distance covered by wild-type control larvae ($p < 10^{-3}$, Wilcoxon test). In comparison, Msp-$300^{\Delta KASH}$ 48 h AEL old larvae will at best cover 30 % of the distance made by controls (Fig. 2a). ens^{swo} larvae present thus an altered locomotion in both L3 [40] and 48 h AEL old larvae (this work) and their locomotion phenotype is milder than the Msp-$300^{\Delta KASH}$ phenotype. Metzger et al. measure the nuclear localization defect by quantifying the distance between neighboring nuclei. This method detects fine nuclei localization defects but does not allow comparison with our measures of nuclei clustering. We therefore evaluated nuclei clustering in ens^{swo} third-instar larval muscles (Fig. 7b). Myonuclei are indeed not as regularly spaced in ens^{swo} third-instar larval muscles as in WT muscle (not shown). However, we did not observe any nuclei clustering in ens^{swo} larvae. We thus concluded that in ens^{swo} mutants, if myonuclei are not evenly spaced as in the wild type, there is no nuclei clustering as observed in Msp-$300^{\Delta KASH}$ mutants. Finally, we looked at Msp-300 subcellular localization in ens^{swo} larvae (in grey,

Fig. 7c–e). Concerning Z-band Msp-300 localization, we did not observe any difference between WT and *ens^swo* larvae. However, we observe a marked modification of Msp-300 perinuclear staining: while in WT muscles myonuclei are directly apposed to the sarcomeres with few and discrete Msp-300 "filaments" contacting them (see Figs. 1c, d, 7c), myonuclei in *ens^swo* muscle are surrounded by a stream of unpatterned Msp-300 staining (Fig. 7d). In addition, in some fibers, the perinuclear regions lack Msp-300 staining (Fig. 7e), a phenotype very similar to Msp-300 localization defects observed in *Msp-300^ΔKASH* mutants.

In conclusion, *ens^swo* larvae have a milder locomotion phenotype than *Msp-300^ΔKASH* larvae, do not show nuclei clustering, although myonuclei are not as evenly spaced as in WT larvae, and present a clear alteration of Msp-300 localization. In light of these observations, it is thus not possible to discriminate between the contributions of Msp-300 and of nuclei fine position in the locomotion phenotype. The absence of nuclei clustering together with the locomotion phenotype observed in *ens^swo* larvae, however, suggests that nuclei clustering itself is not responsible for *Msp-300^ΔKASH* locomotion impairment.

Discussion

In this work, we describe a new and unexpected role of *Drosophila* Nesprin-1, Msp-300, in neuromuscular junction function. We first showed that larvae carrying a deletion of Msp-300 KASH domain present a locomotion defect suggestive of a myasthenia, and demonstrate the importance of muscle Msp-300 for this phenotype, using tissue-specific RNAi knock-down. We then showed that *Msp-300^ΔKASH* mutants display abnormal neurotransmission at the larval neuromuscular junction, as well as an imbalance in postsynaptic glutamate receptor composition with a decreased percentage of GluRIIA-containing receptors. Finally, we could rescue *Msp-300^ΔKASH* locomotion phenotypes by GluRIIA overexpression, suggesting that the locomotion defects associated with the KASH domain deletion are partly due to a reduction in junctional GluRIIA.

Msp-300 is a *bona fide* Nesprin-1

Here we present biological evidence supporting previous bioinformatics prediction that Msp-300 is a Nesprin-1, thus validating the use of *Drosophila* to study LINC complex and Nesprin-1-related diseases. We show that Msp-300 forms filaments with a "beads on a string" pattern, which seems to assemble as sheets at the level of Z-discs and form a web closely apposed to nuclei. This perinuclear localization requires the presence of the KASH domain ([39], this work), showing that the predicted KASH is functional. We

further document a strong nuclear clustering associated with the KASH domain deletion, in agreement with nuclei anchoring defects recently reported by Elhanany-Tamir et al. [39] in larvae carrying a genomic deletion removing the 3prime half of *Msp-300* gene. Nesprin-1 was shown to be an important player of nuclear positioning in mouse muscles, where the KASH domain deletion causes nuclei mislocalization with the occurrence of extrasynaptic nuclei clustering [4, 12] and in *C. elegans* hypoderm syncitia, where loss of the Nesprin-1 homolog ANC-1 causes nuclei clustering [27]. These observations therefore constitute biological evidence that Msp-300 is a *bona fide* Nesprin-1.

Interestingly, Z-disc localization is not affected by the KASH domain deletion. The antibody used in this work was generated using a partial cDNA of Msp-300 [14]. Blast analysis reveals that this cDNA 3' end aligns with all Msp-300 isoforms, the 5' end being shared by fewer isoforms. Msp-300 localizations observed here are thus likely to result from the superposition of several discrete localization patterns corresponding to different isoforms. We propose that KASH-containing isoforms are responsible for the perinuclear Msp-300 staining while the Z-disc staining corresponds to a different subset of Msp-300 isoforms, which could perform different tasks in the cell.

Nuclei clustering and locomotion impairment are disconnected phenotypes

Nuclei clustering is a striking feature of KASH domain deletion in proteins such as Msp-300/Nesprin1 (this work, [4, 11, 41]), ANC-1 [27] and Klarsicht [39]. Correlation between nuclei clustering and locomotion impairment in *Syne-1* KO mice [13], *klarsicht*, and *Msp-300* mutants ([39], this work) together with the occurrence of nuclei abnormal localization in pathologies such as centronuclear myopathies [42] raise the question of the possible contribution of nuclei clustering to the locomotion phenotype. Since we lacked *Msp-300* mutants presenting a locomotion/junctional phenotype without nuclei clustering, therefore establishing the contribution of Msp-300 alone, we decided to examine mutant conditions perturbing nuclear localization and presenting locomotion impairment and ask if these phenotypes occur independently of Msp-300. *klarsicht* mutations result in nuclei clustering and locomotion impairment but also Msp-300 mislocalization. They thus could not be used to discriminate between a role of nuclei clustering or an independent contribution of Msp-300 to the locomotion phenotype. On the other hand, *ens^swo* mutants present altered locomotion ([40], this work), Msp-300 mislocalization (this work), together with irregularly spaced nuclei [40], but no nuclei clusters (this work). Based on these results, we cannot exclude a contribution of fine nuclei position to the locomotion phenotype. However, the

locomotion defects together with the Msp-300 subcellular mislocalization observed in both *ens^swo* and *Msp-300^ΔKASH* larvae independently of the presence or absence of nuclei clusters suggest that nuclei clustering itself is not responsible for the locomotion impairment and rather point toward a direct contribution of Msp-300 localization.

Msp-300 KASH domain deletion alters GluRIIA abundance at the neuromuscular junction

Msp-300^ΔKASH larvae present a clear locomotion defect, which is fully recapitulated in larvae with muscle-specific knock-down of Msp-300 KASH-containing isoforms. We show that this locomotion defect can be explained by a decreased percentage of GluRIIA-containing receptors at the NMJ. Indeed, deletion of one copy of the *gluRIIA* gene results in identical locomotion defects while overexpression of GluRIIA in *Msp-300^ΔKASH* rescues the locomotion phenotype.

When performing electrophysiological analysis, we detected a decrease in eEJC's amplitude and quantal content in *Msp-300^ΔKASH* larvae but no alteration of the mEJCs. This result was at first surprising knowing that these mutant larvae have a decreased GluRIIA density and that GluRIIA density somehow controls mEJPs amplitude. Indeed, increasing GluRIIA density by twofold in GluRIIB null background leads to an increase in mEJP amplitude [31]. According to our immunostainings, GluRIIA density was only decreased by 35 % in *Msp-300^ΔKASH* larvae when compared to WT conditions. Thus, we propose that in *Msp-300^ΔKASH* larvae, the density of postsynaptic GluRIIA-containing receptors is sufficient to give a normal response to the spontaneous exocytosis of one neurotransmitter containing vesicle, hence the lack of modifications in the mEJCs. We also propose that the amount of GluRIIA-containing receptors would be limiting upon stimulation and release of several quanta of neurotransmitter, resulting in decreased eEJCs. This hypothesis is further supported by the observation that although larvae carrying a single copy of the *gluRIIA* gene (*gluRIIA^AD9^/+*) present a clear locomotion defect (similar to *Msp-300^ΔKASH* larvae), larvae with a single copy of both *gluRIIA* and *gluRIIB* genes only present a small decrease in mEJPs [30].

Both the GluR density measures and the electrophysiological analysis are thus in agreement with Msp-300 KASH domain deletion resulting in a decreased postsynaptic sensitivity to neurotransmitter release.

Investigations on the mechanisms underlying GluR synaptic localization have revealed that A- and B-type receptor localization are governed by different processes. Indeed, Discs-Large, a prototypical MAGUK protein localized in the subsynaptic reticulum (SSR), positively regulates B-type receptor NMJ targeting, without affecting A-type receptors [36] while A-type, but not B-type, receptor targeting is under the control of Dorsal (NF-κB) and Cactus (IκB) [38, 43]. We have shown that neither Dorsal nor Cactus SSR localization are affected by Msp-300 KASH domain deletion. We can therefore conclude that Msp-300 contributes to A-type GluR NMJ localization independently of either Dorsal or Cactus.

Several non-mutually exclusive hypotheses can be proposed to explain how Msp-300 KASH domain deletion alters GluR composition at the NMJ.

Disconnecting Msp-300 from the nuclei could directly impact transcription of GluR subunits. Indeed, an increasing number of results suggest that the LINC complex controls gene expression: the LINC complex has been involved in chromatin organization in mammalian cells [7, 24, 44] and *S. cerevisiae* [45] and disconnecting the LINC complex from the actin cytoskeleton leads to altered cellular response to mechanical stress and abnormal gene expression [46–49]. Msp-300 could also control GluR subunit proteins levels by controlling mRNAs access to the translation machinery or post-translational modification of GluRIIA. In agreement with this, human glutamate receptors undergo important post-translational modifications impacting their activity, trafficking, or localization [50]. Similar modifications could occur on GluRIIA and control the assembly of functional postsynaptic glutamate receptors, their activity or localization at the synapse.

Is Msp-300 an organizer of the perinuclear region?

Msp-300 size (13,000 aa for the CH and KASH domain-containing isoforms), the presence of numerous spectrin repeats (up to 52), the localization pattern we observe at Z-band and in the cytoplasm surrounding nuclei (this work), suggest that Msp-300 could be a scaffold organizing the perinuclear region. Several lines of evidence support that hypothesis, which could explain the phenotypes described in this work for *Msp-300^ΔKASH* mutants.

In higher eukaryotes, ER is seen as a highly dynamic continuum consisting of three different subcompartments, the rough ER, the smooth ER, and the nuclear envelope [51]. ER dynamics is thought to play an important role in both the morphology and the functions of ER, and relies mostly on microtubules in mammals and *Drosophila* [52–54]. Elhanany-Tamir et al. [39] documented ER and microtubule organization in WT *Drosophila* larval muscle and showed that astral microtubules are attached to the nuclear envelope from which they radiate, while ER localizes around myonuclei and at Z-bands. This organization is lost in *Msp-300* mutants. In *Msp-300^ΔKASH* mutants, microtubules detach from the nucleus and form a loose perinuclear ring overlapping with Msp-300 ring. Elhanany-Tamir et al. further report an important disorganization of ER

staining in *Msp-300-3prime* deletion mutants. Considering microtubules' important role in ER dynamics and shaping and their disorganization in Msp-$300^{\Delta KASH}$, it is tempting to speculate that ER dynamics or fine subcellular organization might be altered upon Msp-300 KASH domain deletion.

Syne-1, mammalian Msp-300, was isolated in a screen for Golgi-specific spectrin repeats containing proteins [55]. Observation of the subcellular localization of Syne-1 [23] and Golgi [56] in myoblasts and myotubes, together with comparison of physical distance between nuclei and Golgi apparatus and Syne-1 size, led Beck [57] to postulate that Syne-1 could physically couple Golgi, ER, and nuclei in muscle cells.

We therefore speculate that altering Msp-300 anchorage to nuclei could directly impact both ER and Golgi organization and localization with respect to myonuclei or dynamics, thus resulting in altered translation or post-translational modification of proteins including glutamate receptors. Modification of organelle subcellular organization upon Msp300 mutation could thus in turn impact NMJ function.

Finally, Nesprin-1 was originally isolated in a yeast two-hybrid screen for MuSK interactors and called Syne-1 (for synaptic nuclear envelope-1) based on its enrichment at the nuclear envelope of synaptic nuclei [23]. MuSK is a receptor tyrosine kinase involved in acetylcholine receptors clustering at the NMJ in mammals. Although acetylcholine receptor density or molecular architecture of the NMJ are not altered by the expression of a dominant negative form of Syne-1 in transgenic mice [11], effects of Syne-1 KASH domain deletion on NMJ organization were not described. Further investigation is thus necessary to exclude a potential contribution of Syne-1 to NMJ organization. The parallel between the potential involvement of Syne-1 together with MuSK in the clustering of the acetylcholine receptors and the role of Msp-300 in type-A glutamate receptor density at NMJ should nevertheless be kept in mind when investigating the molecular mechanisms of Msp-300/Nesprin-1 contribution to synapse function.

Drosophila NMJ, a relevant model to study Nesprin-linked synaptic diseases

Mutations in Nesprin-1 have been associated with autosomal recessive cerebellar ataxia (ARCA1), EDMD, and autosomal recessive arthrogryposis diseases.

ARCA1 is a neural disorder associated with cerebellar atrophy and impaired walking. Seven mutations were identified in ARCA1 patients, either in introns or exons, leading to a premature stop and resulting in Nesprin-1 C-terminus deletion [58]. These were interestingly associated with mislocalized subsynaptic nuclei at the NMJ [6]. Autosomal recessive arthrogryposis is a rare disease associated with congenital contractures. Analysis of two generations of a congenital family led to the identification of a mutation in *nesprin-1* gene also resulting in a premature stop of the protein and deletion of its KASH domain [59]. Finally, EDMD has been associated with mutations in *LMNA*, *EMD*, and *nesprin-1* and *2* genes, all proposed to affect LINC complex organization [7]. These three pathologies are associated with impaired muscle function, attributed either to neuromuscular or neuronal defects. In all cases, the *nesprin-1* mutations identified result in Nesprin-1 disconnection from the LINC complex, often due to the KASH domain loss, explaining the increasing interest for the contribution of the LINC complex in muscle and neural functions.

In the present study, we show that Msp-$300^{\Delta KASH}$ larvae display obvious signs of locomotion defects that are not due to a lack of muscle contractility but rather to a defective synaptic function. Indeed, our results establish that Msp-300 is involved in the control of glutamate receptor density at the NMJ in a KASH-dependent manner. Considering the role of Msp-300 in controlling postsynaptic homeostasis, it is tempting to speculate that EDMD, ARCA1 and autosomal recessive arthrogryposis could all result from alterations of the postsynaptic fields associated with Nesprin-1 mutations.

Since *Drosophila* NMJ, being glutamatergic, is widely used as a model for central glutamatergic synapses, we propose that *Drosophila* is a new relevant model to study the function of Nesprin-1 in the accumulation of postsynaptic glutamate receptors and more generally to decipher the mechanisms by which Nesprin-1 impacts synapse physiology and understand its implications in neuromuscular and neuronal pathologies.

References

1. Razafsky D, Zang S, Hodzic D (2011) unLINCing the nuclear envelope: towards an understanding of the physiological significance of nuclear positioning. Biochem Soc Trans 39:1790–1794

2. Starr DA (2009) A nuclear-envelope bridge positions nuclei and moves chromosomes. J Cell Sci 122:577–586

3. Wang N, Tytell JD, Ingber DE (2009) mechanotransduction at a distance: mechanically coupling the extracellular matrix with the nucleus. Nat Rev Mol Cell Biol 10:75–82

4. Zhang X, Xu R, Zhu B, Yang X, Ding X, Duan S, Xu T, Zhuang Y, Han M (2007) Syne-1 and Syne-2 play crucial roles in myonuclear anchorage and motor neuron innervation. Development 134:901–908

5. Zhang X, Lei K, Yuan X, Wu X, Zhuang Y, Xu T, Xu R, Han M (2009) SUN1/2 and Syne/Nesprin-1/2 complexes connect centrosome to the nucleus during neurogenesis and neuronal migration in mice. Neuron 64:173–187

6. Gros-Louis F, Dupre N, Dion P, Fox MA, Laurent S, Verreault S, Sanes JR, Bouchard JP, Rouleau GA (2007) Mutations in SYNE1 lead to a newly discovered form of autosomal recessive cerebellar ataxia. Nat Genet 39:80–85

7. Zhang Q, Bethmann C, Worth NF, Davies JD, Wasner C, Feuer A, Ragnauth CD, Yi Q, Mellad JA, Warren DT et al (2007) Nesprin-1 and -2 are involved in the pathogenesis of Emery–Dreifuss muscular dystrophy and are critical for nuclear envelope integrity. Hum Mol Genet 16:2816–2833

8. Emery AE (2000) Emery–Dreifuss muscular dystrophy—a 40-year retrospective. Neuromuscul Disord 10:228–232

9. Sanes JR, Lichtman JW (2001) Induction, assembly, maturation and maintenance of a postsynaptic apparatus. Nat Rev Neurosci 2:791–805

10. Schaeffer L, de Kerchove d'Exaerde A, Changeux JP (2001) Targeting transcription to the neuromuscular synapse. Neuron 31:15–22

11. Grady RM, Starr DA, Ackerman GL, Sanes JR, Han M (2005) Syne proteins anchor muscle nuclei at the neuromuscular junction. Proc Natl Acad Sci USA 102:4359–4364

12. Puckelwartz MJ, Kessler E, Zhang Y, Hodzic D, Randles KN, Morris G, Earley JU, Hadhazy M, Holaska JM, Mewborn SK et al (2009) Disruption of nesprin-1 produces an Emery–Dreifuss muscular dystrophy-like phenotype in mice. Hum Mol Genet 18:607–620

13. Zhang J, Felder A, Liu Y, Guo LT, Lange S, Dalton ND, Gu Y, Peterson KL, Mizisin AP, Shelton GD et al (2010) Nesprin 1 is critical for nuclear positioning and anchorage. Hum Mol Genet 19:329–341

14. Volk T (1992) A new member of the spectrin superfamily may participate in the formation of embryonic muscle attachments in *Drosophila*. Development 116:721–730

15. Zhang Q, Ragnauth C, Greener MJ, Shanahan CM, Roberts RG (2002) The nesprins are giant actin-binding proteins, orthologous to *Drosophila melanogaster* muscle protein MSP-300. Genomics 80:473–481

16. Dietzl G, Chen D, Schnorrer F, Su KC, Barinova Y, Fellner M, Gasser B, Kinsey K, Oppel S, Scheiblauer S et al (2007) A genome-wide transgenic RNAi library for conditional gene inactivation in *Drosophila*. Nature 448:151–156

17. Rohrbough J, Pinto S, Mihalek RM, Tully T, Broadie K (1999) latheo, a *Drosophila* gene involved in learning, regulates functional synaptic plasticity. Neuron 23:55–70

18. Feng Y, Ueda A, Wu CF (2004) A modified minimal hemolymph-like solution, HL3.1, for physiological recordings at the neuromuscular junctions of normal and mutant *Drosophila* larvae. J Neurogenet 18:377–402

19. Marrus SB, Portman SL, Allen MJ, Moffat KG, DiAntonio A (2004) Differential localization of glutamate receptor subunits at the *Drosophila* neuromuscular junction. J Neurosci 24:1406–1415

20. Bolte S, Cordelieres FP (2006) A guided tour into subcellular colocalization analysis in light microscopy. J Microsc 224:213–232

21. Pfaffl MW (2001) A new mathematical model for relative quantification in real-time RT-PCR. Nucleic Acids Res 29:2003–2007

22. Rosenberg-Hasson Y, Renert-Pasca M, Volk T (1996) A *Drosophila* dystrophin-related protein, MSP-300, is required for embryonic muscle morphogenesis. Mech Dev 60:83–94

23. Apel ED, Lewis RM, Grady RM, Sanes JR (2000) Syne-1, a dystrophin- and Klarsicht-related protein associated with synaptic nuclei at the neuromuscular junction. J Biol Chem 275:31986–31995

24. Zhang Q, Skepper JN, Yang F, Davies JD, Hegyi L, Roberts RG, Weissberg PL, Ellis JA, Shanahan CM (2001) Nesprins: a novel family of spectrin-repeat-containing proteins that localize to the nuclear membrane in multiple tissues. J Cell Sci 114:4485–4498

25. Zhang Q, Ragnauth CD, Skepper JN, Worth NF, Warren DT, Roberts RG, Weissberg PL, Ellis JA, Shanahan CM (2005) Nesprin-2 is a multi-isomeric protein that binds lamin and emerin at the nuclear envelope and forms a subcellular network in skeletal muscle. J Cell Sci 118:673–687

26. Xie X, Fischer JA (2008) On the roles of the *Drosophila* KASH domain proteins Msp-300 and Klarsicht. Fly 2:74–81

27. Starr DA, Han M (2002) Role of ANC-1 in tethering nuclei to the actin cytoskeleton. Science 298:406–409

28. Brand AH, Perrimon N (1993) Targeted gene expression as a means of altering cell fates and generating dominant phenotypes. Development 118:401–415

29. Kim K, Lee YS, Harris D, Nakahara K, Carthew RW (2006) The RNAi pathway initiated by Dicer-2 in *Drosophila*. Cold Spring Harb Symp Quant Biol 71:39–44

30. Petersen SA, Fetter RD, Noordermeer JN, Goodman CS, DiAntonio A (1997) Genetic analysis of glutamate receptors in *Drosophila* reveals a retrograde signal regulating presynaptic transmitter release. Neuron 19:1237–1248

31. DiAntonio A, Petersen SA, Heckmann M, Goodman CS (1999) Glutamate receptor expression regulates quantal size and quantal content at the *Drosophila* neuromuscular junction. J Neurosci 19:3023–3032

32. Qin G, Schwarz T, Kittel RJ, Schmid A, Rasse TM, Kappei D, Ponimaskin E, Heckmann M, Sigrist SJ (2005) Four different subunits are essential for expressing the synaptic glutamate receptor at neuromuscular junctions of *Drosophila*. J Neurosci 25:3209–3218

33. Featherstone DE, Rushton E, Rohrbough J, Liebl F, Karr J, Sheng Q, Rodesch CK, Broadie K (2005) An essential *Drosophila* glutamate receptor subunit that functions in both central neuropil and neuromuscular junction. J Neurosci 25:3199–3208

34. Schuster CM, Ultsch A, Schloss P, Cox JA, Schmitt B, Betz H (1991) Molecular cloning of an invertebrate glutamate receptor subunit expressed in *Drosophila* muscle. Science 254:112–114

35. Sigrist SJ, Reiff DF, Thiel PR, Steinert JR, Schuster CM (2003) Experience-dependent strengthening of *Drosophila* neuromuscular junctions. J Neurosci 23:6546–6556

36. Chen K, Featherstone DE (2005) Discs-large (DLG) is clustered by presynaptic innervation and regulates postsynaptic glutamate receptor subunit composition in *Drosophila*. BMC Biol 3:1–13f

37. Cantera R, Kozlova T, Barillas-Mury C, Kafatos FC (1999) Muscle structure and innervation are affected by loss of Dorsal in the fruit fly, *Drosophila melanogaster*. Mol Cell Neurosci 13:131–141

38. Heckscher ES, Fetter RD, Marek KW, Albin SD, Davis GW (2007) NF-kappaB, IkappaB, and IRAK control glutamate receptor density at the *Drosophila* NMJ. Neuron 55:859–873

39. Elhanany-Tamir H, Yu YV, Shnayder M, Jain A, Welte M, Volk T (2012) Organelle positioning in muscles requires cooperation between two KASH proteins and microtubules. J Cell Biol 198:833–846

40. Metzger T, Gache V, Xu M, Cadot B, Folker ES, Richardson BE, Gomes ER, Baylies MK (2012) MAP and kinesin-dependent nuclear positioning is required for skeletal muscle function. Nature 484:120–124

41. Lei K, Zhang X, Ding X, Guo X, Chen M, Zhu B, Xu T, Zhuang Y, Xu R, Han M (2009) SUN1 and SUN2 play critical but partially redundant roles in anchoring nuclei in skeletal muscle cells in mice. Proc Natl Acad Sci USA 106:10207–10212

42. Jungbluth H, Wallgren-Pettersson C, Laporte J (2008) Centronuclear (myotubular) myopathy. Orphanet J Rare Dis 3:26

43. Chen K, Merino C, Sigrist SJ, Featherstone DE (2005) The 4.1 protein coracle mediates subunit-selective anchoring of *Drosophila* glutamate receptors to the postsynaptic actin cytoskeleton. J Neurosci 25:6667–6675

44. Puckelwartz MJ, Kessler EJ, Kim G, Dewitt MM, Zhang Y, Earley JU, Depreux FF, Holaska J, Mewborn SK, Pytel P et al (2010) Nesprin-1 mutations in human and murine cardiomyopathy. J Mol Cell Cardiol 48:600–608

45. Bupp J, Martin AE, Stensrud ES, Jaspersen SL (2007) Telomere anchoring at the nuclear periphery requires the budding yeast Sad1-UNC-84 domain protein Mps3. J Cell Biol 179:845–854

46. Lammerding J, Schulze PC, Takahashi T, Kozlov S, Sullivan T, Kamm RD, Stewart CL, Lee RT (2004) Lamin A/C deficiency causes defective nuclear mechanics and mechanotransduction. J Clin Invest 113:370–378

47. Lammerding J, Hsiao J, Schulze PC, Kozlov S, Stewart CL, Lee RT (2005) Abnormal nuclear shape and impaired mechanotransduction in emerin-deficient cells. J Cell Biol 170:781–791

48. Brosig M, Ferralli J, Gelman L, Chiquet M, Chiquet-Ehrismann R (2010) Interfering with the connection between the nucleus and the cytoskeleton affects nuclear rotation, mechanotransduction and myogenesis. Int J Biochem Cell Biol 42:1717–1728

49. Mejat A, Decostre V, Li J, Renou L, Kesari A, Hantai D, Stewart CL, Xiao X, Hoffman E, Bonne G et al (2009) Lamin A/C-mediated neuromuscular junction defects in Emery-Dreifuss muscular dystrophy. J Cell Biol 184:31–44

50. Qiu S, Li X-Y, Zhuo M (2011) Post-translational modification of NMDA receptor GluN2B subunit and its roles in chronic pain and memory. Sem Cell Dev Biol 22:521–529

51. Voeltz GK, Rolls MM, Rapoport TA (2002) Structural organization of the endoplasmic reticulum. EMBO Rep 3:944–950

52. Pendin D, McNew JA, Daga A (2011) Balancing ER dynamics: shaping, bending, severing, and mending membranes. Curr Opin Cell Biol 23:435–442

53. Park SH, Blackstone C (2010) Further assembly required: construction and dynamics of the endoplasmic reticulum network. EMBO Rep 11:515–521

54. Frescas D, Mavrakis M, Lorenz H, Delotto R, Lippincott-Schwartz J (2006) The secretory membrane system in the *Drosophila* syncytial blastoderm embryo exists as functionally compartmentalized units around individual nuclei. J Cell Biol 173:219–230

55. Gough LL, Fan J, Chu S, Winnick S, Beck KA (2003) Golgi Localization of Syne-1. Mol Biol Cell 14:2410–2424

56. Lu Z, Joseph D, Bugnard E, Zaal KJ, Ralston E (2001) Golgi complex reorganization during muscle differentiation: visualization in living cells and mechanism. Mol Biol Cell 12:795–808

57. Beck KA (2005) Spectrins and the Golgi. Biochim Biophys Acta 1744:374–382

58. Dupre N, Gros-Louis F, Chrestian N, Verreault S, Brunet D, de Verteuil D, Brais B, Bouchard JP, Rouleau GA (2007) Clinical and genetic study of autosomal recessive cerebellar ataxia type 1. Ann Neurol 62:93–98

59. Attali R, Warwar N, Israel A, Gurt I, McNally E, Puckelwartz M, Glick B, Nevo Y, Ben-Neriah Z, Melki J (2009) Mutation of SYNE-1, encoding an essential component of the nuclear lamina, is responsible for autosomal recessive arthrogryposis. Hum Mol Genet 18:3462–3469